NUMERICAL AND EXPERIMENTAL CHARACTERIZATION OF A NON-PREMIXED TURBULENT FLAME

Luis Enrique Alva Huapaya, luisalva@aluno.puc-rio.br
Luís Fernando Figueira da Silva, luisfer@puc-rio.br
Luis Fernando Alzuguir Azevedo, lfaa@puc-rio.br
Pontifícia Universidade Católica do Rio de Janeiro, PUC-Rio

Abstract. *This work presents an experimental and numerical study a non-premixed turbulent flame on a simple geometrical configuration. This flame, which burns natural gas and air, is stabilized downstream to a bluff-body. Initially, literature is reviewed onselected previous experimental studies which have been performed on this kind of burner. Then, the mathematical formulation of computational fluid dynamic problem is presented. This is followed by the introduction of the experimental measurements techniques which involve planar laser induced fluorescence (PLIF). The experimental results were obtained for three combustion regimes, which are characterized by laser induced fluorescence emission of the hydroxil radical species (OH). This characterization involves the analysis the instantaneous and the average structure of the turbulent flame. Finally, the modeling results are compared to the experimental data obtained. This comparison in evidences the necessity to perform the simultaneous measurement of velocity and chemical species concentration in order to allow for the development of new models of combustion in turbulent flows*

Keywords*: Laser induced fluorescence, combustion, turbulence*

1. INTRODUCTION

Until 1998 natural gas had a minor contribution in the Brazilian energy matrix, corresponding to 2.7% of the total generated energy only. According to the forecast of consumption data, presented in the most recent Brazilian energy balance, the participation of the natural gas will evolve from 9,6% in 2006 to circa 12% in 2010. (Ministry of Energy and Mines, 2007). Furthermore, the use of this energy source in replacement to oil leads to improvements, in terms of energy efficiency and environmental impact, since the combustion products of natural gas are the cleanest amongst the fossil fuels. As a consequence of the recent restrictions in pollutant emissions due to environmental regulations, also, it is expected that ever increasing amounts of natural gas will be used in different segments of the industry, such as refineries, metallurgical, ceramics and textile. Combustion in turbulent flows is the common basic process to all these industrial applications, since it can be found in gas turbines, diesel engines, burners, spark ignition engines and furnaces.

The main objective of the present work is to present the results of an experimental and modeling study of non-premixed turbulent flame on a simple geometrical configuration. This flame, which burns natural gas and air, is stabilized downstream to a bluff-body. This simple geometrical configuration allows to decrease of computation effort involved in modeling. Another advantage of this burner is to allow for ample optical access, which facilitaties the detailed characterization of the flow by means of laser-based techniques. The numerical study is conducted using a classical computational fluid dynamics technique.

The planar laser induced fluorescence (PLIF) technique is used in order to characterize the presence of a chemical species (OH) which is present during the combustion process. This paper first presents a literature review of the characterization of bluff body type burners, followed by a brief discussion of the modelling and experimental methodologies. The operation regimes of the burner are discussed, with emphasis on structure of the reactive flow. Then, the obtained experimental and numerical results of OH radical fluorescence are compared for different combustion regimes.

2. BIBLIOGRAPHICAL REVIEW

The nonpremixed bluff body stabilized flame has been extensively studied due the representative nature with respect to industrial applications and to the advantages when addressing the of mixing and combustion processes (Dally et al. 1998). Average flame behavior and the corresponding thermal structures of nonpremixed circular-disk stabilized flames have been studied by Huang and Lin (1994) using direct and schlieren photography techniques. A shown in Fig. 1, the flames were classified in seven characteristic modes:

I Recirculated flame,
II Transition flame,
III Unsteady flame,
IV Laminar ring flame,

V Developing flame,
VI Split flashing flame,
VII Lifted flame
The detailed flow structures and turbulence properties of the combusting flows were examined for different central to annular jet velocity ratio, which was found to influence the flame characteristics. Velocity fields were measured for the different flow regimes with a two component Laser Doppler Velocimeter (LDV) by Huang and Lin (2000), thus allowing to relate the modifications of the flow field to the overall flame structure. Gu et al. (2006) performed an experimental study to determine the effect of humidity on the flow field and the flame stability limit in turbulent nonpremixed flame. The dynamical behavior of the unsteady aerodynamic flow structures on a bluff-body burner was examined for both humid and dry air combustion. Particle image velocimetry (PIV) was used to capture the instantaneous of vortex structures and obtain the velocity field. Figure 1a corresponds to characteristic flames modes observed when the air flow velocity is smaller than 6m/s, whereas in Fig. 1b shows the high-velocity flame structures. The recirculated flame, type I, is characterized by fuel rich combustion. As the central fuel jet velocity is increased (region II), the base of the recirculated flame becomes unstable. In region III, the unsteady detached flame is formed. The flame base is completely detached from the circular disc and combustion is violently unsteady, accompanied by strong puffing noise. In region IV the unsteady detached flame is abruptly stabilized and reattached to the circular disc. The flame in this region is stable and puffing noise disappears.

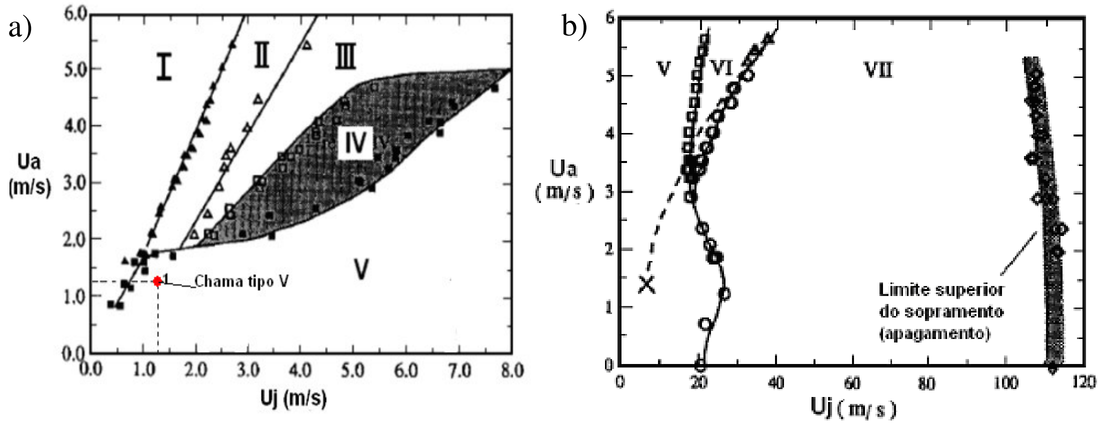

Figure 1 Flame type identification in low (a) and high (b) velocity domains by Huang and Lin (1994).

In the region V a blue neck is formed immediately downstream of the apex of the recirculated soot radiating orange zone. Downstream of the blue neck, the flame is luminous orange. As the central fuel jet velocity is increased to region VI, the orange luminous soot in the recirculation bubble in mode V disappears. A small blue flame stabilized on the circular disc can be found. In region VII the flame ressembles a lifted diffusion flame. Figure 2 shows the flame stabilization domains determined by Gu et al. (2006) in the humid air combustion. Regimes I, II, III and IV correspond to recirculation zone flame, transition flame, central-jet dominated flame and partially quenched flame, respectively. The jet-like flame and lifted flame have not been observed due to insufficiently high fuel velocity.
According to the visual observation of the flame shapes, three stable flame modes are found, as shown in Fig.3. The flame illustrated in Fig. 3a is the recirculation zone flame, which involves complete fuel consumption within the recirculation zone. It is clear that the forward stagnation point is formed in the recirculation zone due to the low central jet momentum. As the fuel-to-air velocity ratio is increased, the reaction within the recirculation zone dominates the flame, and the central jet marginally penetrates the recirculation zone, as illustrated in Fig. 3b. Hence, this flame is called transition flame, and only one stagnation point is observed in the apex area of the recirculation bubble, where the reverse airflow and the central jet mix strongly (Huang and Lin, 1994). When most of the central fuel penetrates the recirculation zone, thus further reducing the vortex strength, the classical central-jet dominated flame is formed. The air and the fuel mix strongly in vicinity of the recirculation zone and a blue neck is formed. Further downstream the flame which may be reignited, is controlled by the nonpremixed flame, as can be seen in Fig. 3c.

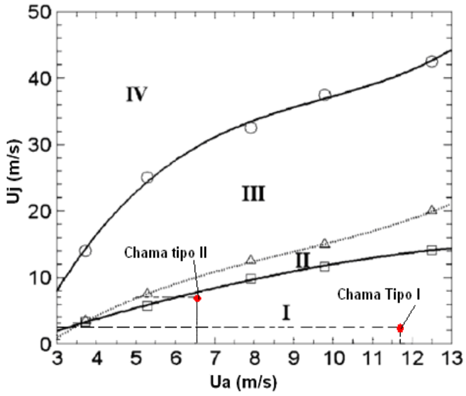

Figure 2 Stabilization regime diagram for humid air combustion Region I recirculation zone flame, Region II transition flame, Region III central-jet dominated flame, Region IV partially quenched flame (Gu et al, 2006).

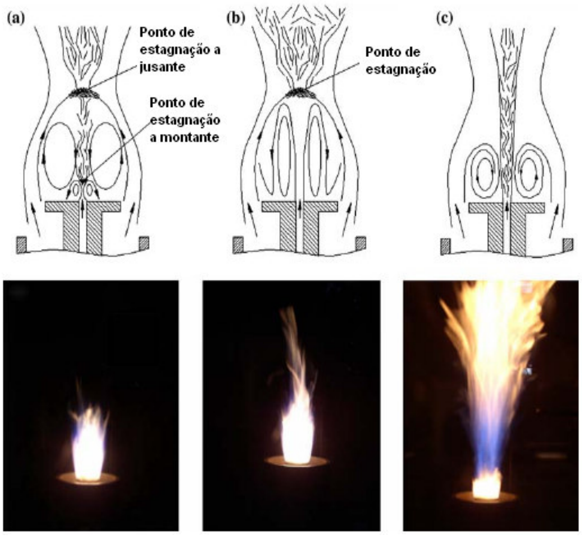

Figure 3 Flame structure for humid air combustion, a) recirculation zone flame, b) transition flame, c) central jet dominated flame (Gu et al. 2006).

3. EXPERIMENTAL SETUP

Figure 4 shows on overall view the combustion system, whose details can be found elsewhere (Alva Huapaya 2008). The fuel (natural gas) jet diameter is 7,1mm, air output diameter 200 mm and bluff body diameter 60 mm. The feed system of air includes a settling chamber downstream to the fan and upstream to the bluff body, which is attached to its base.

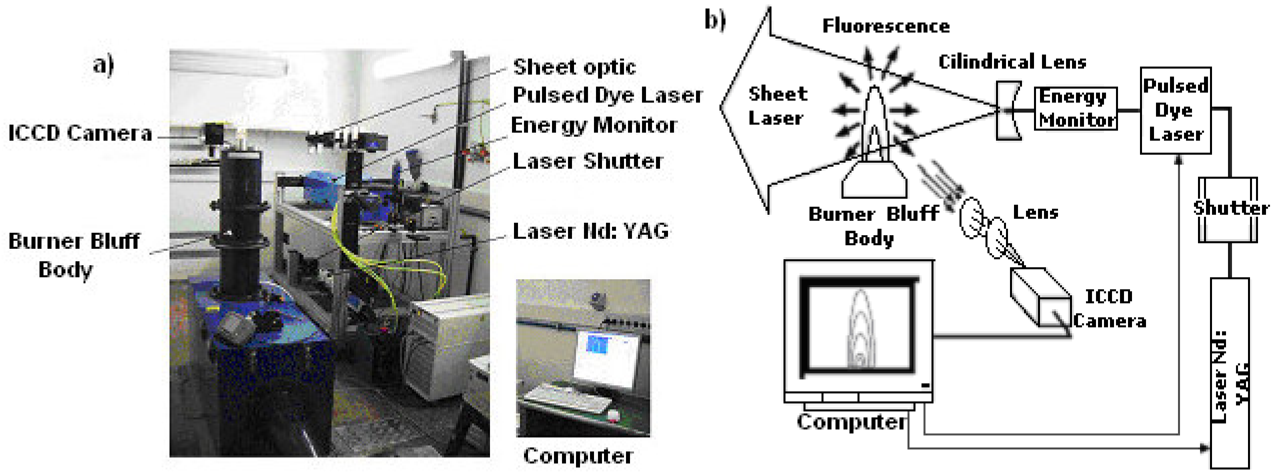

Figure 4 Experimental configuration for the PLIF (a) burner and PLIF system (b) Schematics of the PLIF system

4. NUMERICAL METHODOLOGY

In this work it is assumed that the the reactive flows is governed by the balance equations of mass momentum and energy. The studied flows are transient, compressible and turbulent mixtures of perfect gases. Turbulence is modeled using the classic k-ε and combustion is acconted for by using a Flamelet model (Borghi and Champion, 2000). These equations were solved using classical discretization techniques present in the CFX-10 code. Figure 5 shows scheme of the computational domain and the associated boundaries, which are numbered for the sake of identification. The computational domain is a prism which includes a 15°circular section of the burner. The mesh includes a fuel entrance channel in order to allow a better description of the flow in the vicinity of the face of the burner. A refined region of 60x 40mm^2 in directions x and y, respectively, is included in the mesh, which progressively coarsens away from the burner face.

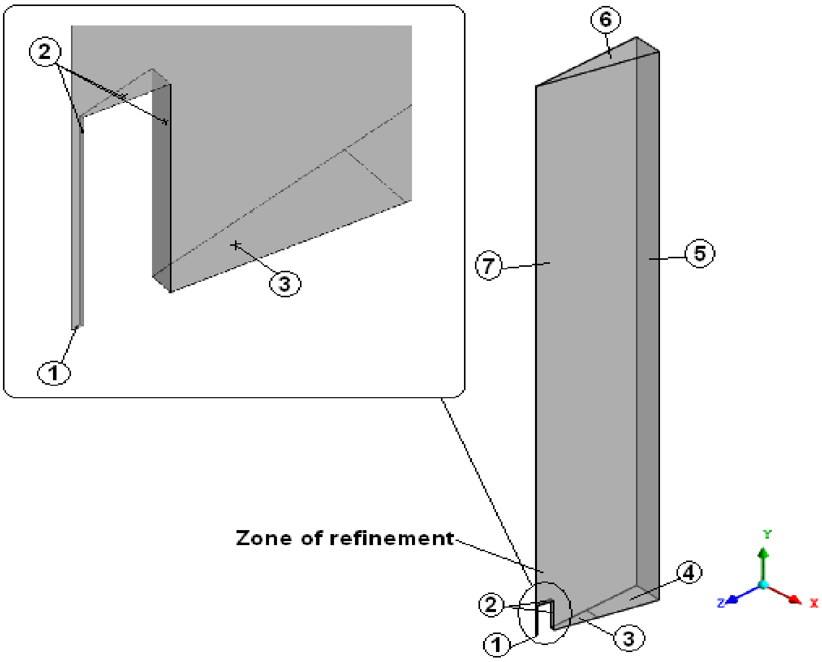

Figure 5 Computational domain with numbered boundary conditions : 1 Section of fuel exit; 2 Face of bluff body burner; 3 annular air inlet; 4 e 5 Boundary condition type “opening”defined as the region where the fluid can cross the boundary in both the directions; 6 Flow outlet; 7 Symmetry Plane.

5. EXPERIMENTAL METHODOLOGY

Laser-based techniques are capable of remote, non-intrusive, in-situ, spatially and temporally accurate measurements of chemical parameters. Such a capability is particularly interesting in the case of combustion processes which may be easily disturbed by sampling techniques. The planar laser-induced fluorescence (PLIF), a derivative of the LIF technique, uses a laser sheet from a probe laser beam in order to excite fluorescence of selected species. This process requires an accurate tuning of laser light in order to excite electronic transitions in the given chemical species. In this work the OH radical is the chosen species which will be characterized by its fluoresce emission at an excitation wavelength of 283,557nm Q1(6) transition of the A–X(1–0) band. The OH fluorescence from the (0, 0) and (1, 1) bands near 310 nm was captured by an intensified CCD camera. The emitted fluorescence light is focused onto an intensified charge-coupled device (ICCD) camera to produce an image of the fluorescence in that region. The basic arrangement of PLIF is given in Fig. 4a. The excitation laser beam passes through a cylindrical lens and transforms into a laser sheet. The laser sheet spreads across the flame produced by the bluff body burner, where it excites the OH radical, causing it to emit fluorescence. A filter and an imaging lens are placed in front of the ICCD to filter and focus the signals. The images captured by the ICCD are transmitted to a computer for processing.
The Nd:YAG Brilliant-B laser used may generate the fundamental wavelength, 1064 nm, or its harmonics (532 nm, 355 nm, 266 nm, 213 nm). The pulse duration at 1064 nm is of 5,64 ns and repetition rate is 10 Hz. The average laser pulse energy is 260 mJ/pulse at the 355 nm harmonic which was used to pump a Sirah model CSTR-G-3000. The dye used is ethanol diluted with at a coumarin 153concentration of 1,6g/l. The purpose of the dye laser is to allow a continuous sweep of wavelengths bands, where chemical species may be excited. An ICCD camera model FM3S with High speed IRO (Intensified relay optics) 1376x1040 pixel of resolution, 70μm by pixel, with the filter bandpass M52 mounted onto, is placed at a right angle to the laser sheet. This filter was selected so that only the fluorescence light passes. S20

photo cathode used allows gate times of typically 100ns. The electronic allows high repetition gating, at frequencies up to 2MHz. The gate pulse widths of the gating electronics is 30ns. The software used to control the lasers, cameras, trigger the various signal was DaVis 7.2. For each laser pulse the relative light intensity was recorded along with the image, so that different images could be compared on a post processing stage. Furthermore, on a given image, each measured pixel intensity, was corrected for the light sheet thickness which was obtained using using the Rayleigh scattering signal resulting from polarizing the laser with a polarization rotator. Another correction employed was the subtration of the CCD background noise. This allows to decrease the systematic errors of the intensity measurement. As the result of such a measurement process, OH fluorescence intensity was obtained for sets of 1000 images for each experimental condition. Correlating intensity to OH concentration would require the use of a canonical calibration flame. This will be subject of future work.

6. RESULTS AND DISCUSSION

After presenting an a priori classification of the flames, a comparison is performed of the overall flame strutures in terms of direct imaging and of instantaneous and averaged OH fluoresence intensity. Then, model and experimental results are compared. In the discussion that follows the flame front position will be considered identical to that of the region of maximum OH intensity.

6.1. Classification of the studied flames

Among the different flame types characterized by Huang and Lin (1994, 2000) and Gu et al. (2006) three representative types are studied in the present work. These three flame types summarized in fig.1a and 2 are (i) type V for Uj=1,35m/s and Ua=1,24m/s, (ii)type I, for Uj=2,19m/s and Ua=11,7m/s, (iii) type II for Uj=6,9m/s and Ua=6,6m/s.

6.2. Average and instantaneous structure

Direct photography, typical instantaneous OH fluorescence images and the corresponding average are shown in figs. 6,7 and 8 for flame types V,I and II, respectively. Figure 6 shows that instantaneous flame front presents only small disturbances with respect to the average position and could be considered quasi-laminar. Indeed, even if average image of figure 6 is not identical to the instantaneous, a similarity can be clearly perceived. The analysis of photographs of this flame types show that as the velocity of fuel jet increases, the length and amplitude of the fluctuations of the visible flame increases. This behavior classical (Lewis and von Elbe, 1987) of type I flames. The comparison between figs 6 and 7 allows to verify the drastic change of flame structure when flow velocity is modified. The structure of each of the instantaneous flames is different, and do not ressemble the average image. The instantaneous flame front is characterized by variable thickness and the presence of regions whose curvature is of the same order of magnitude as the flame thickness. The flame front also shows interruption signals, which suggests the existence of regions where combustible and air mixes in absence of combustion. These modifications of the flame front structure are characteristic of the interaction of combustion and turbulence (Poinsot T., Veynante D. 2005, Borghi R., Champion M. 2000).

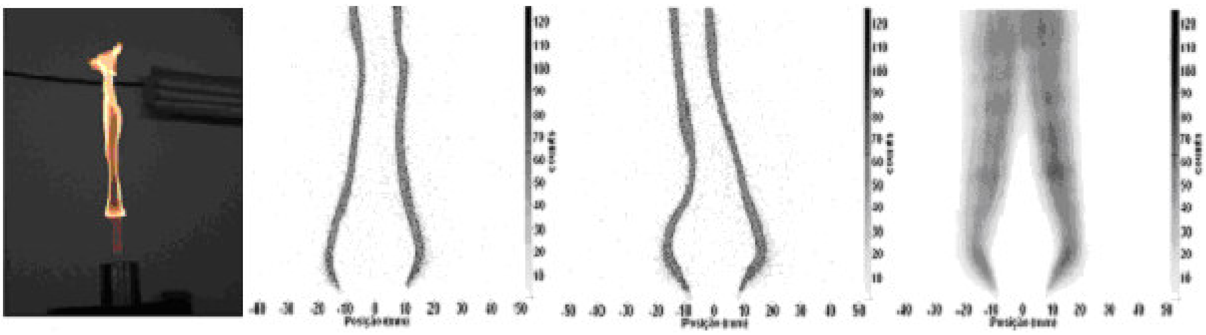

Figure 6 Photograph (exposure time 1ms) instantaneous images of the OH fluorescence intensity and corresponding average image of the flame type V.

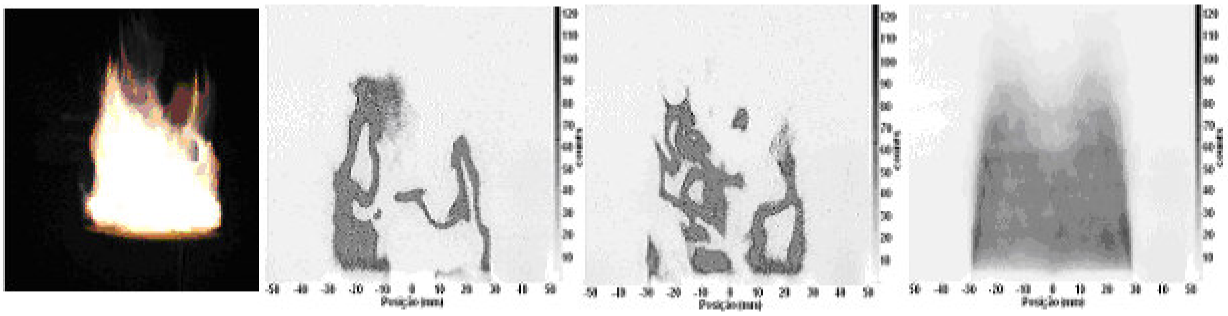

Figure 7 Photograph (exposure time 1ms) instantaneous images of the OH fluorescence intensity and corresponding average image of the flame type I

In the case of the flame type II, which results are presented in fig. 8, the instantaneous flame is strongly bent and interrupted, and thus bears a similarty with type I . However the instantaneous flame is most often detached from the face of the from the burner. Furthermore, there is a clear indication that the fuel jet partly burns away from the burner surface both on the instantaneous and averaged images, due to the reduced OH signal at the burner centerline.
A comparison the average OH intensities shown in figs 7 and 8 shows a distinct change of OH evolution with the distance to the burner face. In type I flames OH intensity decreases with this distance, whereas in type II flames OH exhibits a non-monotonic behavior, first increasing then decreasing with height above the burner. In the former case, it can be expected that the fuel fully burns within the recirculation region, as opposed to the latter, where combustion seems to occur mostly downstream to the expected position of the recirculation region.

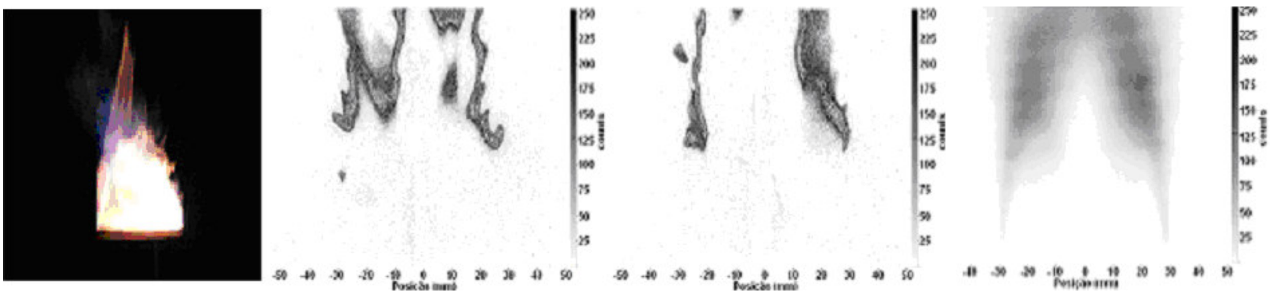

Figure 8 Photograph (exposure time 1ms) instantaneous images of the OH fluorescence intensity and corresponding average image of the flame type II.

6.3. Comparison between modeling and experiment

In this section the experimentaly obtained results of the OH radical fluorescence intensity are compared to the numerical simulation, which uses a flamelet combustion model. This comparison considered the three representative flame types discussed in the preceeding section. Figures 8,9 and 10 show the averaged OH fluorescence intensity and mass fraction radial evolutions at different heights above the burner corresponding to flame types V, I and II, respectively. In the modeling it is supposed that the flame is symmetrical, a hypothesis that is not entirely verified in the experiments, as can be verified in these figures. Nevertheless, the observed a simmetry is sufficiently small so that comparisons can be performed. In fig. 9a it can be observed that the thickness of the OH intensity layer increases from 10 to 20mm when the height varies from 10 to 60mm, although the thickness of the instantaneous laminar flame does not change with the height. This is an indication of the increase of the turbulent intensity with height above the burner. Also, the average flame surface seems be closed at Y=50mm, indicating that, in this area, the fuel was, in average, consumed, which is not obvious from the exam of the instantaneous images shown in fig. 6. The simulation results shown in fig.9b also exhibit a thickness increase with the height, but the flame front closing is not observed. Furthermore, the average flame thickness, 20mm, is practically constant and the OH mass fraction increases up to Y=30mm, and then slightly decreases with the height. This is a consequence of the flame anchoring not being correctly predicted by the modelling. Indeed, in the experiments, the stabilization occurs at the neighborhood of the fuel jet exit, whereas, in the modelling, combustion is stabilized at the the outer rim of the bluff body. Such an incorrect prediction of flame stabilization, which remains to be explained, is at the origin of the disagreement between modeling and experiment results.

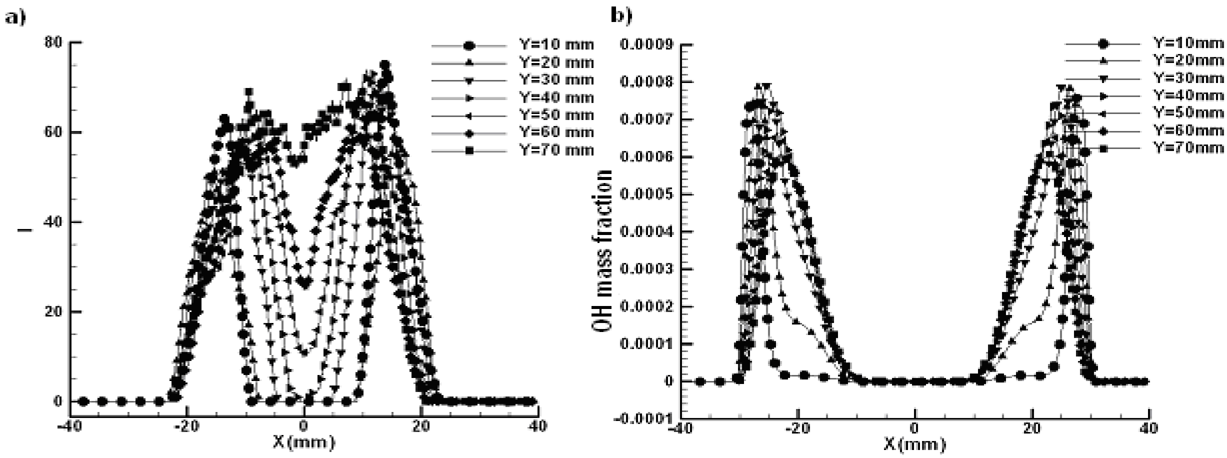

Figure 9 Between experimental and modeled radial evolutions for type V flame (a)measured OH fluorescence intensity (b)computed OH mass fraction.

The model results show a better agreement with respect to the experiments in the case of type I flame, as can be verified in Fig. 9. Indeed, flame attachment, which now occurs at the burner outer rim, is correctly predicted. Furthermore, although a detailed comparison is precluded due to the lack of a correspondence between intensity and mass fraction, the computed trends agree well with the measurement. Indeed, fig. 9 allows to verify that, in the neighborhood of the obstacle, the thickness of average flame front is similar in the experiments and in the modeling. This indicates that the hypothesis of laminar flame elements allows a good description for the interaction between combustion and turbulence even in the presence of local instantaneous flame extinction and wrinkling, as shown in Fig. 7. Further downstream, experimental results and modelling present small discrepancies. In the current state of the analysis of the results, the origin of such a discrepancy could be due either to the inhability of the model in reproducing the phenomena related to extinctions and re-ignitions instantaneous flames or to the incapacity of the models based on the Boussinesq hypothesis of modeling the Reynolds stresses in the presence of rotation and, heat release and consequently, the turbulent transport within the flame.

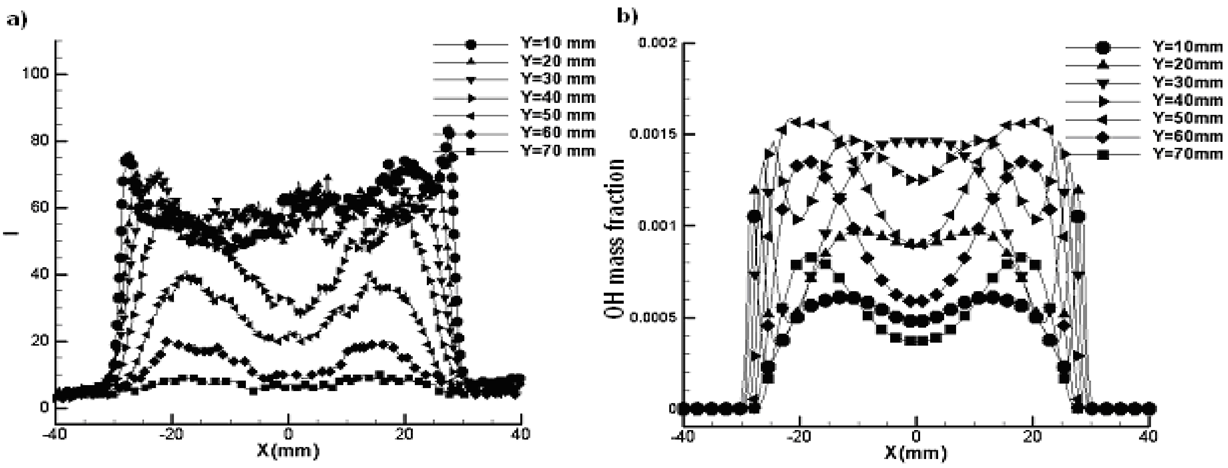

Figura 10 Between experimental and modeled radial evolutions for type I flame (a)measured OH fluorescence intensity (b)computed OH mass fraction.

Flame type II represents a transition unstable situation in which the instantaneous flame front may be alternatively anchored to the face of the burner or detached. Figure 11 indicates that a good agreement exists between modelling and experiment at the neighborhood of the face of the burner. However, the experimental the radial evolution of OH fluorescence intensity indicates that the flame front is closed along the centerline at a height of about 70mm above the burner face, whereas in the simulation it such a closing is not observed, further downstream, the OH intensity is found to remain nearly constant. A different picture is the outcome of the modelling, since the OH mass fraction is practically zero at the centerline. The origins of such a discrepancy are currently under scrutinity.

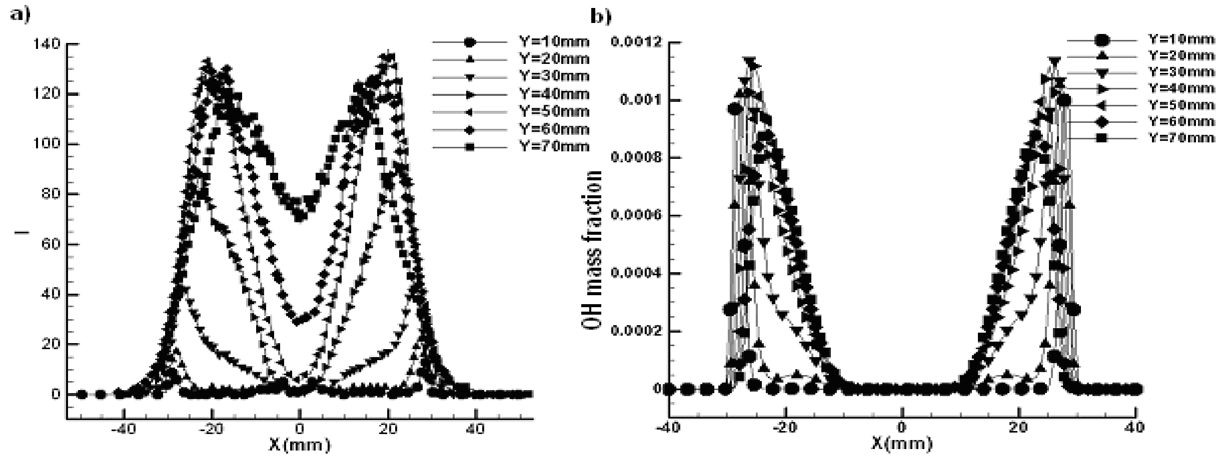

Figure 11 Between experimental and modeled radial evolutions for type II flame (a)measured OH fluorescence intensity (b)computed OH mass fraction.

7. CONCLUSIONS

This work shows the results of the characterization of non premixed turbulent flames of natural gas and air. Three types of flames studied were in agreement with the classification proposed by Huang and Li (1994, 2000) and Gu et al. (2006). Future work will focus on the study of different flame types also.
A non intrusive laser combustion diagnostic technique, PLIF, allowd to study the concentrations of a minor species, characteristic of combustion, the OH radical.
Average image intensity fluorescent of the OH radical obtained for type V flame, show that such flames are dominated by fuel jet. Modeling results exhibit discrepancies with respect to experiments, mostly due to the incorrect prediction of flame anchoring, which is a numerical artifaet which origin is being examined. Successful modeling of the average flame front of the highly wrinkled type I flame was achieved in the vicinity of the burner surface. Discrepancies which may be related to the choice of the eddy-viscosity type turbulence model are observed futher downstream. Even if correct flame anchoring was predicted for flame type II, the extent which combustion penetrates toward the centerline is correct. Current work focus on the use of Reynolds stress tensor models in order to improve turbulence description.

8. ACKNOWLEDGEMENTS

This work was performed while the second author was a visiting researcher with a scholarship from ANP (Agência Nacional do Petróleo, Gás Natural e Biocombustíveis), on leave from Centre National de la Recherche Scientifique (CNRS, France).

9. REFERENCES

ALVA H. L., **Caracterização numérica e experimental de uma chama turbulenta não pré-misturada**. Rio de Janeiro, 169p. Dissertação de Mestrado-Departamento de Engenharia Mecânica, Pontifícia Universidade Católica do Rio de Janeiro. 2008.

BORGHI R., CHAMPION M., **Modélisation et théorie des flammes**, Editions Technip, Paris-França, 2000, 402 p.

CFX 10.0 – **Theory & Tutorial Book**. Ansys Inc, Canada, Ontatio, 2005. http://www.ansys.com/cfx.

DALLY B. B., MASRI A. R., BARLOW R.S., FIECHTNER G. J., **Instantaneous and mean compositional structure of bluff-body stabilized nonpremixed flames**. Combustion and Flame vol. 114, pp 119- 148, 1998.

GU X., ZANG S.S., GE B., **Effect on flow field characteristics in methane-air non-premixed flame with steam addition**, Experiments in Fluids, vol. 41, pp 829-837, 2006.

HUANG R. F., LIN C.L., **Characteristic modes and thermal structure of nonpremixed circular-disc stabilized flames,** Combustion Science and Technology, vol. 100, pp. 123-139, 1994

HUANG R. F., LIN C.L., **Velocity fields of nonpremixed bluff-body stabilized flames**, Jornal of Energy Resources Technology, vol. 122, pp. 88-93, 2000.

LEWIS B.; VON ELBE G. **Combustion, flames and explosions of gases**, 3ed. Orlando, Flo.: Academis Press, 1987. 739p.

MINISTÉRIO DE MINAS E ENERGIA DO BRASIL E EMPRESA DE PESQUISA ENERGÉTICA; **Balanço energético doméstico, 2007** (ano base 2006), Rio de Janeiro 2007, 190 p.

POINSOT T., VEYNANTE D., **Theoretical and numerical combustion**, 2.ed. Editora Edwards R. T., 2005, 520 p.